frontiers in Marine Science

ORIGINAL RESEARCH
published: 17 June 2016
doi: 10.3389/fmars.2016.00099

Distribution and Speciation of Dissolved Iron in Jiaozhou Bay (Yellow Sea, China)

Han Su[1], Rujun Yang[1], Ivanka Pižeta[2], Dario Omanović[2], Shirong Wang[1] and Yan Li[1]*

[1] College of Chemistry and Chemical Engineering, Ocean University of China, Qingdao, China, [2] Division for Marine and Environmental Research, Ruđer Bošković Institute, Zagreb, Croatia

The distribution of total dissolved iron (DFe) and its chemical speciation were studied in vertical profiles of the shallow and semi-closed Jiaozhou Bay (JZB, China) during two contrasting periods: summer (July 19th, 2011) and spring (May 10th, 2012). Samples collected from the surface, middle and bottom layers were analyzed by competitive ligand exchange-adsorptive cathodic stripping voltammetry (CLE-aCSV). The mean DFe concentration during the summer period (median 18.8 nM; average 20.7 nM) was higher than in the spring period (median 12.4 nM; average 16.9 nM), whereas the spatio-temporal variation in spring was larger than in summer. The DFe-values showed distinct regional and seasonal differences, ranging from 5.6 to 107 nM in spring period and 13.4 to 43.4 nM in summer period. In spring, the highest DFe-values were observed in the eastern coastal region, especially near an industrial area (up to 107 nM), whereas the DFe distribution in summer was relatively even. Due to a tide influence, the vertical variations in the DFe and L_t in both seasons were not significant. On average, the L_t concentration (one class of ligand was estimated in all samples), was higher in spring (35.2 ± 23.4 nM) than in summer (31.1 ± 10.3 nM). A statistically significant correlation was found between L_t and DFe concentrations, it was higher for the summer period than for the spring period. The conditional stability constants (logK′) of organic complexes with iron were weaker in spring (11.7 ± 0.3) than in summer (12.3 ± 0.3). The concentrations of L_t were higher in comparison to DFe in all samples: the average $[L_t]/[DFe]$ ratio in the spring and summer samples was 2.4 and 1.5, respectively. Speciation calculations showed that the DFe in the JZB existed predominantly (over 99.99%) in the form of strong organic complexes in both seasons.

Keywords: dissolved iron, organic ligand, horizontal and vertical distribution, speciation, coastal water, the Jiaozhou Bay (JZB)

OPEN ACCESS

Edited by:
Antonio Tovar-Sanchez, Consejo Superior de Investigaciones Científicas, Spain

Reviewed by:
Loes Gerringa, NIOZ-Royal Netherlands Institute for Sea Research, Netherlands
Constant Marius G. Van Den Berg, University of Liverpool, UK

****Correspondence:***
Rujun Yang
yangrj@ouc.edu.cn

Specialty section:
This article was submitted to Marine Biogeochemistry, a section of the journal Frontiers in Marine Science

Received: *31 January 2016*
Accepted: *03 June 2016*
Published: *17 June 2016*

Citation:
Su H, Yang R, Pižeta I, Omanović D, Wang S and Li Y (2016) Distribution and Speciation of Dissolved Iron in Jiaozhou Bay (Yellow Sea, China). Front. Mar. Sci. 3:99. doi: 10.3389/fmars.2016.00099

INTRODUCTION

Iron (Fe) is an essential trace element in marine environments and plays an important role in the biochemistry and physiology of phytoplankton (Martin and Fitzwater, 1988; Sunda et al., 1991). The world's surface HNLC (high nutrient low chlorophyll) oceans area has influenced phytoplankton growth due to low concentration of iron (Coale, 2004). In the 1990's, Martin hypothesized that the low concentration of iron in oceans across the globe limited the absorption

of CO_2 from the atmosphere and subsequently had an important influence on the global climate (Martin, 1990). After that, iron fertilizing experiments were arranged in the HNLC area (Boyd et al., 2007; Buesseler et al., 2008). The results indicated that in the HNLC area, the addition of iron increased the growth of marine phytoplankton and also influenced local CO_2 absorption and nutrient consumption (biogeochemical cycles of carbon, Boyd et al., 2007).

It has been shown that not only low concentrations, but also low bio-availability of dissolved iron may limit the growth of marine organisms (Morel et al., 1991; Sunda et al., 1991; Poorvin et al., 2004). Since ∼99.9% of the dissolved iron (DFe) is complexed by strong organic ligands (Rue and Bruland, 1995; van den Berg, 1995), not all is equally bioavailable. It is known that ligand-complexed iron is available and taken up by organisms, for example eukaryotic phytoplankton assimilating porhyrin-complexed iron and prokaryotes uptaking siderophore-complexed iron (Hutchins et al., 1999). On the other hand, Fe-binding organic ligands (L_t) buffer DFe concentrations by preventing the formation of insoluble oxy-hydroxides (Rue and Bruland, 1995; Wu and Luther, 1995; Kuma et al., 1996; Mawji et al., 2008), because Fe-organic complexes have higher stability constants than inorganic ones (Hudson and Morel, 1993; Nagai et al., 2007). Therefore, the character of L_t plays an important role in the biogeochemical cycles of iron in global open oceans (Buck et al., 2007).

The concentrations of L_t vary widely in marine environment: for open oceans, L_t concentration is low, e.g., 0.44 nM was observed in Indian Sector of the Southern Ocean (Gerringa et al., 2008), 17.6 nM was observed in the Atlantic Sector of the Southern Ocean (Croot and Johansson, 2000), and range from 0.09 to 0.77 nM in Central N Pacific (Rue and Bruland, 1995). In coastal waters, the L_t is higher than in the open ocean, whereas the highest concentrations of L_t were observed in the estuary areas and river plumes [e.g., 526 nM in the Scheldt Estuary; 4.3–64.1 nM in the Mississippi River plume (Powell and Wilson-Finelli, 2003; Gerringa et al., 2007)]. In the coastal area of the East China Sea, the L_t ranged from 5.2 to 132 nM (Su et al., 2015).

The most accepted method for determination of concentrations of L_t and the conditional stability constants ($\log K'$) of metal-organic ligands in marine samples is competitive ligand exchange-adsorptive cathodic stripping voltammetry (CLE-aCSV; Gledhill and van den Berg, 1994; van den Berg, 1995). It is based on titration of the samples with a metal of interest in which competitive ligand is added. One to two ligand classes were usually determined. The speciation analysis results (concentration of accessible organic ligands, L_t, and conditional stability constant, $\log K'$) depend not only on the quality of the experimental titration data, but also on the applied mathematical treatment (Pižeta et al., 2015). In recent studies only one class of ligands was estimated in Liverpool Bay (Abualhaija et al., 2015; Sander et al., 2015) and the Otago Continental Shelf (Sander et al., 2015). However, two classes of organic ligands were often reported in seawater samples, a stronger ligand (L_1; $\log K'_1$) and weaker (L_2) ligand ($\log K'_2$; Rue and Bruland, 1995; Cullen et al., 2006; Buck et al., 2007). The values of $\log K'$ were close to the values obtained by model ligands with organic matter such as siderophores produced by bacteria (Hider and Kong, 2010), porphyrins derived from pigments (Witter et al., 2000), and degradation products from marine and terrestrial organisms, among other humic substances (HS; Laglera and van den Berg, 2009). While interpreting results from CLE-aCSV one should further bear in mind that ligand—DFe coordination could be different from 1:1 ratio, and that not all DFe in a given sample is in an exchangeable form with respect to the added competitive ligand, having as a consequence a possible overestimation of L_t and higher $\log K'$ (Cullen et al., 2006; Thuróczy et al., 2010; Gledhill and Buck, 2012).

The coastal zone is influenced by iron input from river waters, which may be transported a long distance (Powell and Wilson-Finelli, 2003; Su et al., 2015). Rainwater is also a significant source of iron in surface waters (Kieber et al., 2001), especially through rivers collecting drainage water and entering into coastal waters. A factor that may speed-up the depletion of DFe is algal bloom. Marine phytoplankton cells when of high density, would uptake bioavailable iron and decrease the DFe concentration (Boye et al., 2001, 2003). Appearance of anoxia (due to red tide) in bottom water and sediments may cause the release of iron from sediments into surrounding waters (Sundby et al., 1986; Zhu et al., 2012). In coastal areas where monsoons blow, they transport dust and may be another factor that influence the distribution of DFe and L_t, which may lead to seasonal variation in the DFe and L_t, such as Funka Bay (Japan, Tsunogai and Uematsu, 1978) and Arabian Sea (Siefert et al., 1999). In recent years, as the economy has developed, anthropogenic sources such as industrial wastewater, sewage, agriculture irrigation, and other activities influence more and more the biogeochemical cycling of the DFe and L_t in coastal areas.

Due to the limited water exchange, semi-closed bays like Jiaozhou Bay (JZB) are vulnerable marine ecosystems, sensitive to any kind of change or pollution, and could be used to evaluate the contribution of natural and anthropogenic sources on DFe and L_t concentrations on the system itself (Kremling et al., 1997; Öztürk et al., 2003; Nagai et al., 2007).

JZB water body with a surface area of 390 km^2 is connected with the Yellow Sea through a narrow mouth that starts in Tuandao and ends in Xuejiadao with a width of merely 3.1 km (Li et al., 2014; **Figure 1**). The JZB is surrounded by a highly industrialized and populated area, the biggest being Qingdao city, having a total population of ∼8.7 million inhabitants. The eastern coastal JZB is an industrial and residential area, while the western coastal area is mainly an agriculture and aquaculture district. JZB has an average water depth of ∼7 m, shallow in the northwest and deep in the southeast (**Figure 1**; Chen et al., 2009). The average tidal range of JZB is 2.7 m, with a maximum of 6.9 m, inducing strong turbulent mixing (Deng et al., 2010). The amount of river water entering the JZB varies seasonally, more than 10 rivers dry up in the winter and spring seasons but carry a large quantity of anthropogenic contaminants into this area in the rainy summer season (Ma et al., 2014). According to the report on Marine Environmental Quality of Qingdao (2014), red tides happen every year in spring and in summer (Bulletin of Marine Environmental

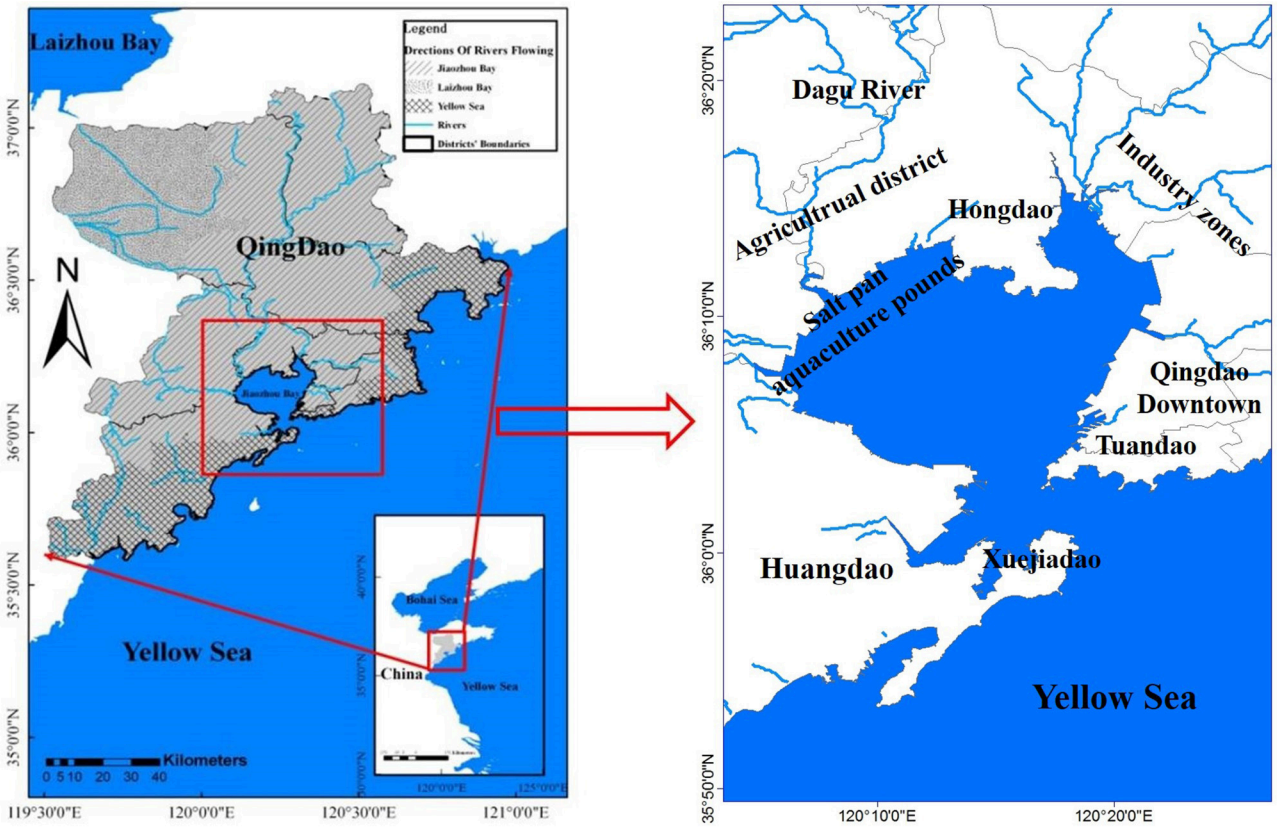

FIGURE 1 | The geographic location of Jiaozhou Bay, Qingdao, China.

Status of China for the year of 2011 and 2012[1]; Liu et al., 2005).

The purpose of this work is to provide an insight into the distribution and speciation of dissolved iron (DFe) and its organic ligands (L_t) in relation to anthropo-biogeochemical changes of the water in the JZB, caused by anthropogenic inputs through the rivers inflow or naturally driven disturbances as a consequence of tide, rain, or increased biological activity.

SAMPLING AND ANALYTICAL PROCEDURES

Samples Collection

Samples were collected during two cruises on a wooden boat in the JZB in summer (July 19, 2011) and spring (May 10, 2012). The sampling stations were located between 120.12–120.35°E and 35.03–36.20°N. The seawater samples were collected from five sections, which were identified as A, B, C, D and E, from each position at three depths (**Figure 2**; note slight differences in positions and number of sampling stations between summer and spring).

[1]http://www.coi.gov.cn/gongbao/huanjing/.

Based on the relative distance to the bay mouth and the different influence from industry and agriculture, the sample stations were classified into three groups:

1. The northwest coastal stations (NWS) having shallow water (~4 m depth, **Figure 2**) and weaker water exchange with the Yellow Sea than other areas of the JZB (Lü et al., 2010). In the NWS area, there are saltpans and aquaculture ponds, such as shrimps and shellfish ponds (Guo et al., 2012; Ma et al., 2014; **Figure 1**). The northern and western coastal districts of JZB are mainly agricultural (Liu et al., 2014).
2. The eastern coastal stations (ES) were near downtown and were deeper than the western and northern JZB stations (**Figure 2**). The eastern coastal area of JZB is industrial with high population density. Different industries are located in this area, including electroplating, metal processing, rubber manufacturing, petrochemistry, machinery manufacturing, etc. (Deng et al., 2010). The rivers (Moshui, Baisha, Loushan, Licun, and Haibo Rivers) in the ES region have become the sewage channels for Qingdao city (**Figure 2**).
3. The central and southern stations (CSS) have the strongest water exchange and tidal influence, along with big topographic relief, slope and submarine depression (**Figure 2**). A narrow channel near the mouth of the

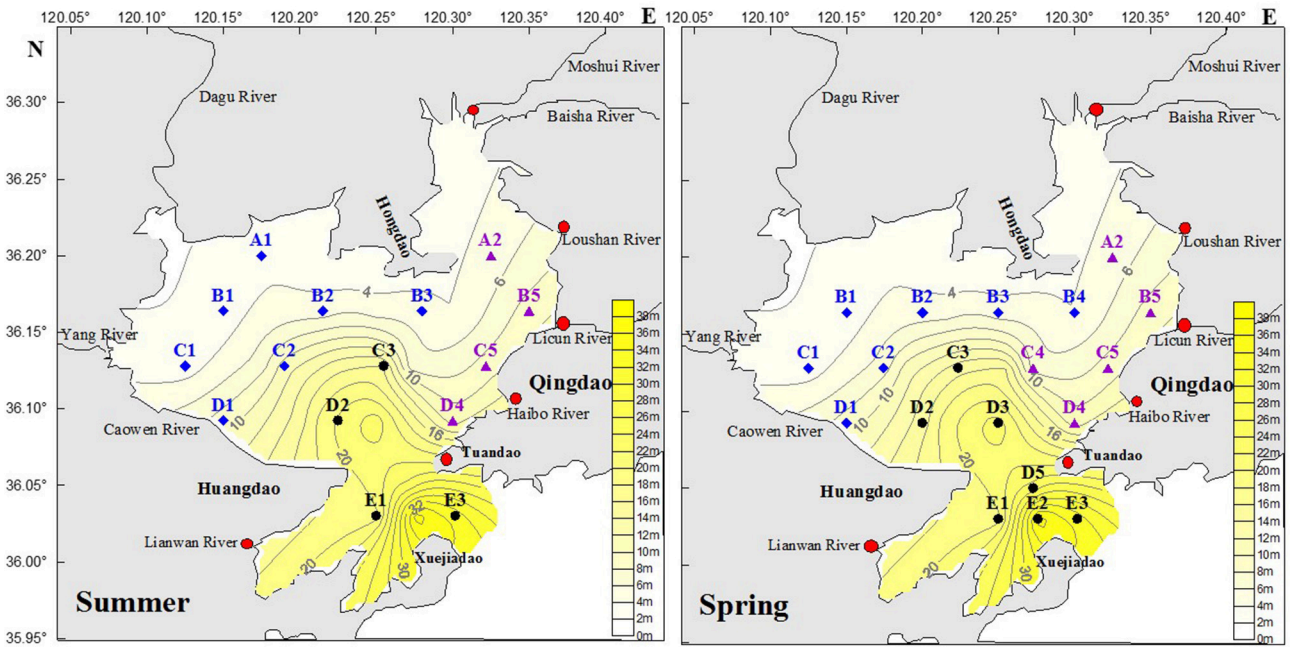

FIGURE 2 | Locations of sampling stations during the summer (July 19, 2011) and the spring cruise (May 10, 2012) in the JZB. Stations are classified into three regions: northwestern coastal stations (region NWS, ◆, in blue), eastern coastal stations (region ES, ▲, in purple), and central and southern stations (region CSS, ●, in black). Gray color represents the depth of the JZB. "●" represents sewage treatment plants discharging into the JZB.

bay is seriously impacted by strong tidal currents (Ding, 1992).

Samples were collected with metal-clean modified Teflon-coated PVC Go-Flo bottles (UPVC/PTFE, 140 × 670 mm, Tianjin, National Ocean Technology Center, China) with a plastic rope. After recovery, the samples were immediately subsampled into 1 L low-density polyethylene bottles (LDPE, Nalgene, USA), and were then pressure-filtered through an acid-cleaned 0.4 μm-pore polycarbonate filter (47 mm × 0.4 μm, Millipore, Ireland). The filtered seawater samples for DFe analysis were collected into three clean 30 ml LDPE bottles (Nalgene, USA), immediately acidified to pH < 2 using HCl (Suprapur, Merck, Germany), and stored for more than 3 months before measurements, then analyzed for DFe concentration. Other filtered seawater samples were collected in a clean 250 mL LDPE bottles and frozen for subsequent analysis of Fe speciation. All of these procedures were performed in a class-100 clean laminar flow bench.

Bottle Washing and Reagents

The sample bottles were washed several times with 10% (v/v) HCl (Guaranteed reagent, Sinopharm, China) and rinsed thoroughly with a Milli-Q water, as described in details by Su et al. (2015). All reagents were made in Milli-Q water (18.2 MΩ, Millipore, USA). The hydrochloric acid (HCl, mass fraction 30%) was ultra-pure grade (Merck, 1.00318.1000, Germany). Ammonium hydroxide was prepared with a vapor-phase transfer from reagent-grade concentrated NH_4OH into ultra-high purity H_2O. A stock standard solution of 1000.0 mg/L $Fe(NO_3)_3$ (chromatographically pure, Merck, Germany) was prepared and diluted to 100, 10, and 1 μM (in pH = 2) to obtain working solutions. The competitive ligand used was 2,3-dihydroxynaphthalene (DHN; chromatographically pure, Merck, Germany), and a stock standard solution of 0.1 M DHN was prepared and diluted to 100 μM. BrO_3^- (0.4 M; BHD, UK)/POPSO (0.1 M; chromatographically pure, Merck, Germany) as a buffer solution was purified using 100 μM MnO_2 (van den Berg, 2006).

Determination of Total Dissolved Iron and Organic Fe-Binding Ligands

The total dissolved iron in acidified seawater samples and organic Fe-binding ligands in thawed samples were determined by CLE-aCSV method and a 797 VA computrace instrument (Metrohm, Switzerland). Detailed information on the determination of DFe and L_t (i.e., electrochemical parameters and the process of determination) were provided elsewhere (van den Berg, 2006; Su et al., 2015). In short, voltammetric parameters were as follows: method differential pulse voltammetry, deposition potential −0.2 V, deposition time 60 s, pulse amplitude 0.05 V, pulse time 0.02 s, scan rate 90 mV/s, initial potential 0.0 V, final potential −1.2 V.

For determination of DFe concentration, 40 μL of 0.01 M DHN and 0.5 mL of BrO_3^-/POPSO was added to a 10 ml of sample to adjust the pH to 8.0–8.1. DFe concentration was determined for every sample in triplicate (from three bottles/subsamples). We added a higher concentration of DHN (40 μM) for the determination of DFe than for the determination of L_t and logK (1.5 μM). For determination of L_t and its iron binding conditional stability constant ($\log K'_{FeL}$), every seawater sample was pipetted into a series of 13 Teflon tubes (Nalgene,

USA) and titrated with at least 10 Fe additions (the range of iron additions: 0, 0.5, 1.0, 2.0, 3.0, 4.0, 6.0, 10.0, 15.0, 20.0, 30.0, 40.0, 50.0, and 70.0 nM) in order to fully saturate all ligand sites. After 30 min equilibration of samples with iron additions, DHN was added to the final concentration of 1.5 μM. These samples were further equilibrated for 12–17 h. Before measurement, Teflon tubes were well-conditioned using an iron solution of the same concentration. Subsequently, equilibrated samples were transferred to a measurement cell, from low to high iron addition aliquots, and measured at pH 8.0–8.1.

The side reaction coefficient (α_{FeDHN}) for 1.5 μM of DHN was calculated by:

$$\alpha_{FeDHN} = K^{cond}_{FeDHN} \times \left[\mathrm{DHN}'\right] = 10^{8.51} \times 1.5 \times 10^{-6} = 485.4$$

For this method $[\mathrm{DHN}'] = [\mathrm{DHN_T}]$, since $[\mathrm{DHN}'] >> [\mathrm{DFe}]$.

The results of each titration set (signal height vs. added Fe concentration) were treated by ProMCC software (Omanović et al., 2015). Sensitivity (S) was adopted from the last five points of titration data. Langmuir/Gerringa non-linear fitting was applied assuming one- and two-ligand models. The one-ligand model was adopted in all cases.

Inorganic Fe (Fe′) of the samples was related to the initial iron reduction peak current, i_{p0}:

$$\left[\mathrm{Fe}'\right] = i_{p0}/(\mathrm{S} \times \alpha_{FeDHN}) \qquad (a)$$

The other way of estimating inorganic Fe, with obtained results from titration experiment, i.e., L_t and logK′ relies on Equation (9) from Omanović et al. (2015):

$$\left[\mathrm{Fe}'\right] = \frac{-\alpha + \sqrt{\alpha^2 + \frac{4[DFe]}{K'}}}{2} \qquad (b)$$

where $\alpha = (-[\mathrm{DFe}] + [\mathrm{L_t}] + 1/\mathrm{K}')$.

The two approaches will be checked and compared. Estimations that take into account parameters of iron complexation with organic ligands (b) should be more reliable, as they are calculated from more data points. From the other side, propagation of errors that is inherent to complex calculations makes the simpler expression (a) also valuable.

The percentage of complexed *DFe (%FeL)* was calculated from:

$$\%FeL = \frac{[DFe] - \left[Fe'\right]}{[DFe]} \times 100\%$$

Temperature, Salinity, and Nutrients Measurements

The surface water temperature was measured *in-situ* at the sampling sites by a digital thermometer with a long probe. The salinity of surface water was measured by a salinometer (SYA2-2, China; calibrated by standard seawater provided by National Center of Ocean Standards and Metrology, Tianjin, China) in for that specified subsamples after coming back to the laboratory. Nutrients levels (total dissolved nitrogen and phosphorus) were measured in the laboratory using spectrophotometry (Grasshoff et al., 1983) after the water was passed through an acid-clean 0.4 μm-pore filter.

RESULTS

Results of all measured and calculated parameters: dissolved iron, calculated and estimated iron-organic ligands parameters, inorganic iron, percentage of organically bound iron as well as temperature, salinity, total dissolved nitrogen, and phosphorus, for both contrasting summer and spring periods, are summarized in **Tables 1, 2**.

Distribution of Dissolved Iron in the JZB

The contour plots of spatial distributions of DFe concentrations in surface, middle, and bottom seawater layers in the JZB in summer period are shown in **Figures 3A–C**. The spatial distributions in all three layers exhibited a weak horizontal gradient, progressively decreasing from the CSS region ([DFe] ranged from 13.4 to 43.4 nM, median 19.8 nM, average ± *SD* 23.7 ± 9.7 nM) to the ES region ([DFe] ranged from 14.8 to 29.8 nM, median 18.7 nM, average ± *SD* 19.5 ± 4.6 nM), and NWS ([DFe] ranged from 13.5 to 32.1 nM, median 17.2 nM, average ± *SD* 19.2 ± 4.9 nM). Although not significant, the vertical profiles of average DFe concentration in all regions showed a decrease with depth.

The spatial distributions of DFe concentrations in the surface, middle and bottom seawater layers during the spring period are shown in **Figures 3D–F**. A strong horizontal decrease in DFe from the eastern to the western and central side of the bay is obvious. The highest variability in [DFe] (from 5.6 to 107 nM; median 9.8 nM, average ± *SD* 24.1 ± 28.3 nM) was observed in the ES region. In the NWS region, [DFe] ranged from 8.3 to 31.4 nM (median 13.5 nM, average ± *SD* 13.6 ± 5.8 nM) and in the CSS region, [DFe] ranged from 8.1 to 26.8 nM (median 14.1 nM, average ± *SD* 14.5 ± 5.5 nM). Similar to the summer period, DFe concentrations decreased with depth in all three layers.

Distribution of Iron Organic Ligands in the JZB

In all samples from the spring and summer periods only one class of Fe-binding ligand was estimated (further in the text denoted as total ligand concentration, $[L_t]$; **Figure 4**).

The spatial distributions of $[L_t]$ in the surface, middle and bottom samples for the summer campaign are shown in **Figures 4A–C**. On average, L_t concentrations were about 50% higher than [DFe], with a statistically significant correlation with ([DFe]; $R^2 = 0.54$, $n = 46$, $p < 0.001$; **Figure 5**). While vertical profiles of $[L_t]$ showed an evident decrease with depth (surface layer: 37.1 ± 10.0 nM; middle layer: 30.4 ± 9.7 nM, bottom layer: 26.3 ± 9.7 nM), the horizontal variation between regions was minor (ES region: 32.0 ± 9.3 nM; NWS region: 31.4 ± 11.0 nM; CSS region: 29.9 ± 10.8 nM). The relatively narrow range of logK′ obtained in all summer samples (12.3 ± 0.4; $n = 46$) revealed an absence of any horizontal or vertical gradients, pointing on the similarity in organic ligand complexation characteristics

TABLE 1 | Dissolved iron DFe (average from three determinations ± standard deviation); iron ligand characteristics L_t, logK′ (± 95% confidence interval determined through fitting to Langmuir/Gerringa model) and [L_t]/[DFe]; inorganic iron (Fe′, pM, both calculated by expression a and b) and the percentage of complexed DFe (%FeL, calculated by expression a) at all stations in spring and summer.

	ID	Dep	[DFe]	[L_t]	logK′	[L_t]/[DFe]	[Fe′] (a)	%FeL (a)	[Fe′] (b)	Dep	[DFe]	[L_t]	logK′	[L_t]/[DFe]	[Fe′] (a)	%FeL (a)	[Fe′] (b)
		(m)	(nM)	(nM)			pM		pM	(m)	(nM)	(nM)			pM		pM
NWS	A1	0	27.3 ± 2.6	54.3 ± 3.0	12.6 ± 0.2	2	0.19	99.999	0.25	–			–	–	–		
		3	16.0 ± 1.2	22.1 ± 0.3	11.8 ± 0.1	1.4	1.33	99.992	4.15	–			–	–	–		
	B1	0	20.6 ± 2.1	30.5 ± 0.6	12.2 ± 0.1	1.5	1.4	99.993	1.31	0	10.2 ± 0.8	17.3 ± 0.5	11.7 ± 0.1	1.7	0.88	99.991	2.86
		2	25.7 ± 1.5	44.3 ± 1.7	12.2 ± 0.2	1.7	0.79	99.997	0.87	2	7.6 ± 0.5	14.0 ± 1.6	11.6 ± 0.1	1.8	0.9	99.988	2.98
		4	17.4 ± 2.4	35.5 ± 1.0	11.8 ± 0.1	2	1.65	99.99	1.52	–			–	–	–		
	B2	0	32.1 ± 3.2	52.6 ± 0.6	12.9 ± 0.4	1.6	0.17	99.999	0.2	0	9.2 ± 1.9	22.4 ± 1.4	12.7 ± 0.3	2.4	0.43	99.995	0.14
		2	14.5 ± 1.3	20.3 ± 1.7	11.6 ± 0.1	1.4	1.08	99.993	6.27	2	9.0 ± 1.1	26.1 ± 0.6	11.6 ± 0.1	2.9	0.88	99.99	1.32
		4	16.6 ± 1.4	25.1 ± 1.6	11.8 ± 0.1	1.5	1.13	99.993	3.09	4	18.0 ± 2.7	27.5 ± 1.3	11.6 ± 0.1	1.5	1.18	99.993	4.76
	B3	0	14.1 ± 1.7	35.6 ± 0.6	12.2 ± 0.2	2.5	0.3	99.998	0.41	0	17.5 ± 1.4	48.1 ± 1.4	11.8 ± 0.1	2.7	0.8	99.995	0.91
		2	15.9 ± 1.4	19.8 ± 0.5	11.7 ± 0.1	1.2	1.48	99.991	8.11	2	17.3 ± 0.7	50.3 ± 0.9	11.6 ± 0.1	2.9	1.21	99.993	1.32
		4	21.4 ± 2.0	26.0 ± 0.4	12.4 ± 0.3	1.2	0.21	99.999	1.85	4	15.2 ± 0.85	22.7 ± 0.7	11.8 ± 0.2	1.5	1.08	99.993	3.21
	B4			–		–	–	–		0	12.0 ± 0.6	54.9 ± 3.8	10.9 ± 0.1	4.6	0.92	99.992	3.52
	C1	0	16.3 ± 2.1	27.9 ± 0.9	12.6 ± 0.2	1.7	0.22	99.999	0.35	0	14.8 ± 2.3	39.5 ± 1.9	11.5 ± 0.1	2.7	1.09	99.993	1.89
		1	14.0 ± 0.9	24.5 ± 0.4	12.6 ± 0.1	1.7	0.27	99.998	0.33	–			–	–	–		
		2	18.7 ± 1.2	36.4 ± 1.4	11.8 ± 0.1	1.9	1.31	99.993	1.67	3	8.3 ± 0.8	14.0 ± 0.9	11.5 ± 0.1	1.7	0.68	99.992	4.6
	C2	0	20.6 ± 1.4	47.8 ± 2.7	12.3 ± 0.1	2.3	0.34	99.998	0.38	0	14.6 ± 1.7	30.4 ± 1.6	11.3 ± 0.1	2.1	0.86	99.994	4.63
		5	21.4 ± 1.6	33.7 ± 1.3	12.7 ± 0.2	1.6	0.23	99.999	0.35	3	14.4 ± 0.4	34.6 ± 3.2	11.2 ± 0.1	2.4	0.78	99.995	4.5
		10	17.1 ± 2.0	19.6 ± 1.3	12.6 ± 0.2	1.1	0.82	99.995	1.72	6	13.5 ± 1.8	42.0 ± 4.5	11.2 ± 0.1	3.1	0.77	99.994	2.99
		–								3	9.5 ± 1.1	35.2 ± 0.7	11.6 ± 0.1	3.7	0.5	99.995	0.93
		–								6	5.6 ± 1.1	14.8 ± 0.5	11.5 ± 0.1	2.6	0.59	99.99	1.92
	D1	0	16.9 ± 1.0	24.2 ± 0.5	12.3 ± 0.2	1.4	1.42	99.992	1.16	0	31.4 ± 3.7	53.4 ± 0.8	12.1 ± 0.2	1.7	0.84	99.997	1.13
		5	23.5 ± 1.3	30.2 ± 0.9	12.2 ± 0.1	1.3	1.81	99.992	2.21	5	9.5 ± 1.7	25.8 ± 1.1	11.5 ± 0.1	2.7	1.16	99.988	1.84
		7	13.5 ± 0.8	18.4 ± 1.0	12.0 ± 0.1	1.4	1.17	99.991	2.75	8	8.3 ± 1.6	21.5 ± 1.0	11.6 ± 0.1	2.6	0.73	99.991	1.58
ES	A2	0	16.3 ± 0.7	24.8 ± 1.5	12.5 ± 0.2	1.5	0.48	99.997	0.61	0	9.8 ± 2.0	21.8 ± 0.6	11.6 ± 0.1	2.2	1.25	99.987	2.05
		2	17.2 ± 1.6	28.2 ± 1.8	12.1 ± 0.1	1.6	0.96	99.994	1.24	2	8.9 ± 2.1	27.4 ± 1.0	11.9 ± 0.2	3.1	0.5	99.994	0.61
		4	15.9 ± 1.7	22.7 ± 0.2	12.2 ± 0.1	1.4	1.05	99.993	1.47	3	9.2 ± 1.9	29.9 ± 0.7	11.8 ± 0.1	3.3	0.61	99.993	0.7
	B5	0	18.6 ± 1.5	43.3 ± 1.8	12.4 ± 0.2	2.3	0.29	99.998	0.3	0	107 ± 2.9	144 ± 3.5	12.2 ± 0.2	1.3	2.25	99.998	1.82

(Continued)

TABLE 1 | Continued

	ID	Dep (m)	[DFe] (nM)	$[L_t]$ (nM)	logK′	$[L_t]$/[DFe]	[Fe′] (a) pM	%FeL (a)	[Fe′] (b) pM	Dep (m)	[DFe] (nM)	$[L_t]$ (nM)	logK′	$[L_t]$/[DFe]	[Fe′] (a) pM	%FeL (a)	[Fe′] (b) pM
		5	20.8 ± 1.4	42.4 ± 2.4	12.3 ± 0.2	2	0.8	99.996	0.48	5	58.9 ± 3.2	104 ± 1.5	11.7 ± 0.1	1.8	2.71	99.995	2.61
		8	21.1 ± 1.0	41.4 ± 2.4	12.3 ± 0.3	2	0.36	99.998	0.52	8	55.5 ± 4.3	109 ± 3.2	11.8 ± 0.1	2	1.41	99.997	1.64
	C4	–								0	9.1 ± 1.5	38.5 ± 1.0	11.3 ± 0.1	4.2	1.2	99.997	1.55
	C5	0	26.4 ± 2.0	41.9 ± 2.3	12.3 ± 0.2	1.6	0.58	99.998	0.85	0	22.3 ± 2.3	40.6 ± 1.2	12.1 ± 0.2	1.8	0.53	99.998	0.97
		5	19.4 ± 2.3	34.3 ± 0.9	12.0 ± 0.1	1.8	1.23	99.994	1.3	5	6.9 ± 1.5	27.2 ± 0.8	11.6 ± 0.1	4	0.52	99.992	0.85
		8	18.9 ± 1.8	28.5 ± 0.4	12.1 ± 0.1	1.5	1.13	99.994	1.56	8	9.4 ± 1.1	45.5 ± 1.5	11.5 ± 0.1	4.9	0.52	99.994	0.82
	D4	0	29.8 ± 2.5	38.0 ± 1.0	12.6 ± 0.3	1.3	0.89	99.997	0.91	0	22.6 ± 1.4	34.3 ± 0.6	11.7 ± 0.1	1.5	2.51	99.989	3.85
		5	14.8 ± 1.0	21.6 ± 2.4	12.2 ± 0.2	1.5	0.78	99.995	1.37	3	12.4 ± 2.0	27.1 ± 0.6	11.7 ± 0.1	2.2	1.31	99.989	1.68
		10	14.8 ± 3.0	17.4 ± 0.7	12.3 ± 0.1	1.2	0.97	99.993	2.85	8	14.6 ± 0.4	40.4 ± 0.6	12.3 ± 0.2	2.8	0.43	99.997	0.28
CSS	C3	0	21.0 ± 1.4	35.2 ± 1.3	13.1 ± 0.3	1.7	1.15	99.995	0.12	0	12.2 ± 1.1	35.1 ± 2.0	10.9 ± 0.1	2.9	1.19	99.99	6.7
		10	17.3 ± 0.8	22.3 ± 1.1	12.3 ± 0.2	1.3	1.25	99.993	1.73	7	10.4 ± 1.1	31.2 ± 1.9	11.5 ± 0.1	3	0.97	99.991	1.58
		15	15.5 ± 0.7	17.7 ± 1.3	12.2 ± 0.1	1.1	1.07	99.993	4.44	14	8.1 ± 0.8	22.5 ± 0.3	11.5 ± 0.1	2.8	0.78	99.99	1.78
	D2	0	25.8 ± 2.0	34.1 ± 1.3	12.7 ± 0.1	1.3	0.85	99.997	0.62	0	11.1 ± 1.7	34.4 ± 0.8	11.8 ± 0.1	3.1	0.66	99.994	0.75
		10	13.4 ± 0.9	14.9 ± 0.6	12.1 ± 0.2	1.1	1	99.992	7.06	7	10.4 ± 1.2	24.5 ± 1.5	11.6 ± 0.1	2.3	0.94	99.991	1.85
		–								14	26.8 ± 2.4	30.6 ± 2.7	11.6 ± 0.1	1.1	2.86	99.989	17.62
	D3	–								0	19.5 ± 2.1	32.0 ± 2.5	12.1 ± 0.3	1.6	0.94	99.995	1.24
		–								10	21.6 ± 1.2	33.8 ± 0.7	12.0 ± 0.1	1.6	1.08	99.995	1.77
		–								20	17.0 ± 1.4	22.2 ± 0.2	11.9 ± 0.1	1.3	1.92	99.999	4.11
	D5	–								0	9.8 ± 1.5	24.8 ± 1.0	11.6 ± 0.1	2.5	1.15	99.988	1.64
		–								10	8.6 ± 1.8	38.1 ± 3.0	11.5 ± 0.1	4.4	0.69	99.992	0.92
		–								20	8.2 ± 1.5	19.3 ± 1.3	11.7 ± 0.1	2.3	0.88	99.989	1.47
	E1	0	19.2 ± 0.9	23.4 ± 2.2	12.9 ± 0.3	1.2	0.57	99.997	0.58	0	9.8 ± 0.3	12.3 ± 2.5	11.2 ± 0.1	1.3	0.95	99.99	24.43
		5	19.9 ± 1.5	24.8 ± 5.6	12.8 ± 0.3	1.2	0.49	99.998	0.64	10	14.1 ± 1.0	28.6 ± 1.1	12.1 ± 0.2	2	0.5	99.996	0.77
		10	17.2 ± 1.9	21.1 ± 3.5	12.1 ± 0.3	1.2	1.09	99.994	3.5	15	15.4 ± 0.8	42.6 ± 1.0	11.7 ± 0.1	2.8	0.88	99.994	1.13
	E2	–								0	22.6 ± 2.1	36.4 ± 1.4	12.1 ± 0.1	1.6	1.08	99.995	1.3
		–								15	15.2 ± 1.7	23.1 ± 1.0	11.5 ± 0.1	1.5	1.39	99.991	6.08
		–								30	23.4 ± 1.2	25.0 ± 0.8	11.8 ± 0.1	1.1	1.61	99.993	22.83
	E3	0	40.4 ± 1.0	42.6 ± 0.3	12.9 ± 0.1	1.1	3.08	99.992	2.31	0	11.3 ± 1.7	15.8 ± 0.6	11.9 ± 0.1	1.4	1.23	99.989	3.16

(Continued)

TABLE 1 | Continued

ID	Dep	[DFe]	[L_t]	logK′	[L_t]/[DFe]	[Fe′]	%FeL	[Fe′]	Dep	[DFe]	[L_t]	logK′	[L_t]/[DFe]	[Fe′]	%FeL	[Fe′]
						(a)	(a)	(b)						(a)	(a)	(b)
	(m)	(nM)	(nM)			pM		pM	(m)	(nM)	(nM)			pM		pM
	5	19.8 ± 2.3	28.5 ± 1.6	12.3 ± 0.1	1.4	1.55	99.992	1.14	15	14.2 ± 1.8	29.1 ± 2.5	12.0 ± 0.1	2.1	0.89	99.994	0.95
	10	43.4 ± 3.0	49.0 ± 1.4	12.1 ± 0.1	1.1	3.42	99.992	6.15	30	14.9 ± 1.7	20.8 ± 3.3	11.9 ± 0.1	1.4	1.63	99.989	3.18
	15	23.5 ± 1.2	33.1 ± 2.5	12.0 ± 0.2	1.4	1.59	99.993	2.45								
	20	18.2 ± 0.8	23.9 ± 3.9	11.9 ± 0.2	1.3	1.23	99.993	4.02								
	25	38.0 ± 2.0	47.4 ± 0.4	12.5 ± 0.1	1.2	1.18	99.997	1.28								
NWS	*Average ± SD*	19.2 ± 4.9	31.4 ± 11.0	12.2 ± 0.4	1.6 ± 0.4	0.9 ± 0.6	99.995	2.0 ± 2.1		13.6 ± 5.8	32.0 ± 13.7	11.6 ± 0.4	2.4 ± 0.8	0.9 ± 0.2	99.993	2.6 ± 1.5
	Median	17.2	29.1	12.2	1.5	0.95	99.994	1.4		13.5	27.5	11.6	2.4	0.88	99.993	2.86
ES	*Average ± SD*	19.5 ± 4.6	32.0 ± 9.3	12.3 ± 0.2	1.6 ± 0.3	0.8 ± 0.3	99.996	1.1 ± 0.7		24.1 ± 28.3	49.3 ± 37.8	11.8 ± 0.3	2.8 ± 1.1	1.1 ± 0.8	99.993	1.5 ± 0.9
	Median	18.7	31.4	12.3	1.6	0.84	99.995	1.08		9.8	35.2	11.7	2.6	0.61	99.994	1.55
CSS	*Average ± SD*	23.7 ± 9.7	29.9 ± 10.8	12.4 ± 0.4	1.3 ± 0.2	1.4 ± 0.8	99.994	2.6 ± 2.2		14.5 ± 5.5	27.7 ± 7.7	11.7 ± 0.3	2.1 ± 0.9	1.2 ± 0.5	99.992	5.0 ± 7.2
	Median	19.8	26.7	12.3	1.2	1.16	99.993	2.02		14.1	28.6	11.7	2	0.97	99.991	1.77

toward Fe in the JZB (**Table 1**). A fairly uniform distribution of DFe organic fraction (>99.99% of FeL) was observed (**Table 1**). However, a distinctly different [L_t]/[DFe] ratio was obtained for the CSS region (1.3 ± 0.2) compared to the ES (1.6 ± 0.3) and NWS (1.6 ± 0.4) regions (**Table 1**). Calculations showed slight variations of inorganic Fe concentrations by region (in average [Fe′] = 1.0 ± 0.7 pM (expression a, $n = 46$) and 1.9 ± 1.9 pM (expression b, $n = 46$) in the whole JZB; **Table 1**). Comparisons of two approaches of inorganic Fe estimation showed good correlation of both estimation in the ES region, while for the NWS and CSS regions, expression b gave higher estimations. The high estimations of inorganic Fe mainly coincident with lower stability constants.

The spatial distributions of [L_t] in the surface, middle and bottom samples for the spring campaign are shown in **Figures 4D–F**. The [L_t] exceeded the [DFe] for all samples and showed a statistically significant correlation with [DFe] ($R^2 = 0.784$, $n = 53$, $p < 0.0001$; **Figure 5**). Similar to summer vertical profiles, the average [L_t] decreased with depth (surface layer: 38.7 ± 28.1 nM; middle layer: 35.4 ± 19.4 nM; bottom layer: 31.4 ± 21.8 nM). Contrary to a uniform horizontal distribution evidenced in summer, in the spring period there were evident differences in L_t between regions (ES: 49.3 ± 37.8 nM; NWS: 32.0 ± 13.7 nM; CSS: 27.7 ± 7.7 nM. On average, lower conditional stability constants (logK′) in the spring period were obtained than in summer period (11.7 ± 0.3; $n = 53$) with no significant differences between the regions (**Table 1**). However, [L_t]/[DFe] ratios in spring were evidently higher than in summer, with a clear difference between regions: ES: 2.8 ± 1.1; NWS: 2.4 ± 0.8; CSS: 2.1 ± 0.8. Similar to summer, organically complexed iron fraction accounted for more than 99.99% of DFe. The calculated concentration of inorganic Fe—in average [Fe′] = 1.1 ± 0.5 pM (expression a, $n = 53$) and 3.2 ± 4.8 pM [expression b, $n = 53$)] did not differ much from the summer period (**Table 1**). Similar to summer period, two estimates of inorganic Fe correlate well for the ES region, while even more extreme values were calculated with expression b especially in the CSS region, where at some locations inorganic Fe was estimated to more than 20 pM. These samples were characterized by low stability constants.

Results from Physical and Chemical Parameters Measurements

The main physico-chemical parameters (temperature and salinity) were measured *in-situ*, at the surface (**Table 2**).

Total dissolved nitrogen (TDN) and phosphorus (TDP) concentrations were determined in all surface samples as well (**Table 2**).

DISCUSSION

Chemical and Physical Parameters and Factors That Influence the Behavior of Iron in the JZB

Salinity of the JZB was influenced by factors such as the tide, freshwater, and salt pans. The tide increases salinity of the JZB, because the Yellow Sea water of higher salinity mixes

TABLE 2 | Temperature (T, °C) and salinity (S), total dissolved nitrogen (TDN, μM) and total dissolved phosphorus (TDP, μM) at the surface layer of each sampling station in summer and spring in the JZB.

Region	Site	Summer period				Spring period			
		T (°C)	*S*	[TDN] (μM)	[TDP] (μM)	*T* (°C)	*S*	[TDN] (μM)	[TDP] (μM)
NWS	A1	24.6	32.1	–	–	–	–	–	–
	B1	24.5	31.6	72.1	0.64	17.2	30.6	52.2	–
	B2	24.2	31.3	84.8	0.98	17.2	30.6	49.5	0.47
	B3	24.4	29.9	92.3	1.07	17.1	30.9	59.6	0.57
	B4	–	–	–	–	17.9	30.5	72.2	1.16
	C1	25.0	31.8	82.1	0.58	17.1	31.4	54.1	0.35
	C2	23.5	30.2	52.0	0.76	15.5	30.9	66.5	0.70
	D1	24.5	29.8	–	–	16.4	30.8	–	0.3
	A2	22.4	30.2	90.1	1.32	18.3	30.8	72.3	1.43
	B5	23.4	29.8	–	–	17.0	30.3	91.2	1.80
	C4	–	–	–	–	15.3	32.2	49.1	0.65
	C5	23.1	30.4	87.1	0.91	16.0	31.0	48.1	0.75
	D4	22.6	31.6	–	0.84	14.3	31.3	41.2	0.42
CSS	C3	22.9	31.7	–	–	14.4	31.6	52.3	0.36
	D2	22.8	32.3	68.2	0.71	14.2	31.1	–	–
	D3	–	–	–	–	14.4	31.3	36.8	0.36
	D5	–	–	–	–	14.6	31.1	39.8	0.39
	E1	22.7	30.7	57.5	0.56	13.4	31.2	30.8	0.34
	E2	–	–	–	–	13.5	31.5	34.0	–
	E3	23.1	30.8	52.2	0.69	14.0	31.1	34.2	0.27
NWS	Avg.	24.4	31.0	76.7	0.81	16.9	30.8	59.0	0.59
ES	Avg.	22.9	30.5	88.6	1.02	16.2	31.1	60.4	1.01
CSS	Avg.	22.9	31.4	59.3	0.65	14.1	31.3	38.0	0.34

Dep (m) represented the depth of sampling. Here, "–" refers to the parameter "not determined" in these analyses.

with freshwater that rivers bring into the bay. Although in the west-northern bay, there are many salt pans, which would increase salinity of the JZB due to their flooding (**Figure 1**), the continuous freshwater mixing with high salinity water at estuaries results in no big variations of salinity that we measured in our study in any of the three regions (**Table 2**).

Total dissolved nitrogen (TDN) and phosphorus (TDP) concentrations in the ES region were higher than in the other two regions (**Table 2**). Industrial wastewater and sewage had the biggest impact on nutrients in the JZB. The ratio of TDN to TDP in spring and summer (87:1 and 88:1, respectively) was much higher than the Redfield ratio (15:1, Redfield, 1958); the TDP may be the main limiting factor of phytoplankton growth in the JZB (Guo et al., 2012), and consequently may influence the distribution of DFe.

Monsoons can disturb surface water and increase dissolved iron deposition from the atmosphere to a surface water (Lin and Twining, 2012), thereby increasing the DFe concentrations of the semi-closed JZB. Due to the proximity to land, a large amount of atmospheric inputs might have contributed to high iron concentrations (Baker et al., 2003). During a monsoon, the influence of atmospheric inputs may be greater than at other times. In our results, the DFe concentrations of surface water in spring were higher than in the middle and bottom water, while this phenomenon was not observed in summer. This might be due to the prevailing northwest monsoon in Qingdao (Tan et al., 2012), especially from March to May when we collected spring seawater samples (**Figure 3**).

Due to the narrow entrance of the JZB, tidal movement induces strong turbulent mixing and nearly homogeneous vertical profiles of temperature and salinity (Ding, 1992) at the bay mouth. This has caused no distinct vertical differentiation of DFe-values, except at station E1 (**Figure 3** and **Table 1**).

DFe of the whole inner bay is not likely to be influenced by sediment resuspension because of bedrock and minimal sediment of the seafloor (Chen et al., 2012a). The river and silt input from rivers would directly increase the DFe concentrations under the tidal movement. Higher river runoff in summer may increase the DFe concentrations more than in spring (**Figures 3**, **6**, see Section Sources and Removal of DFe).

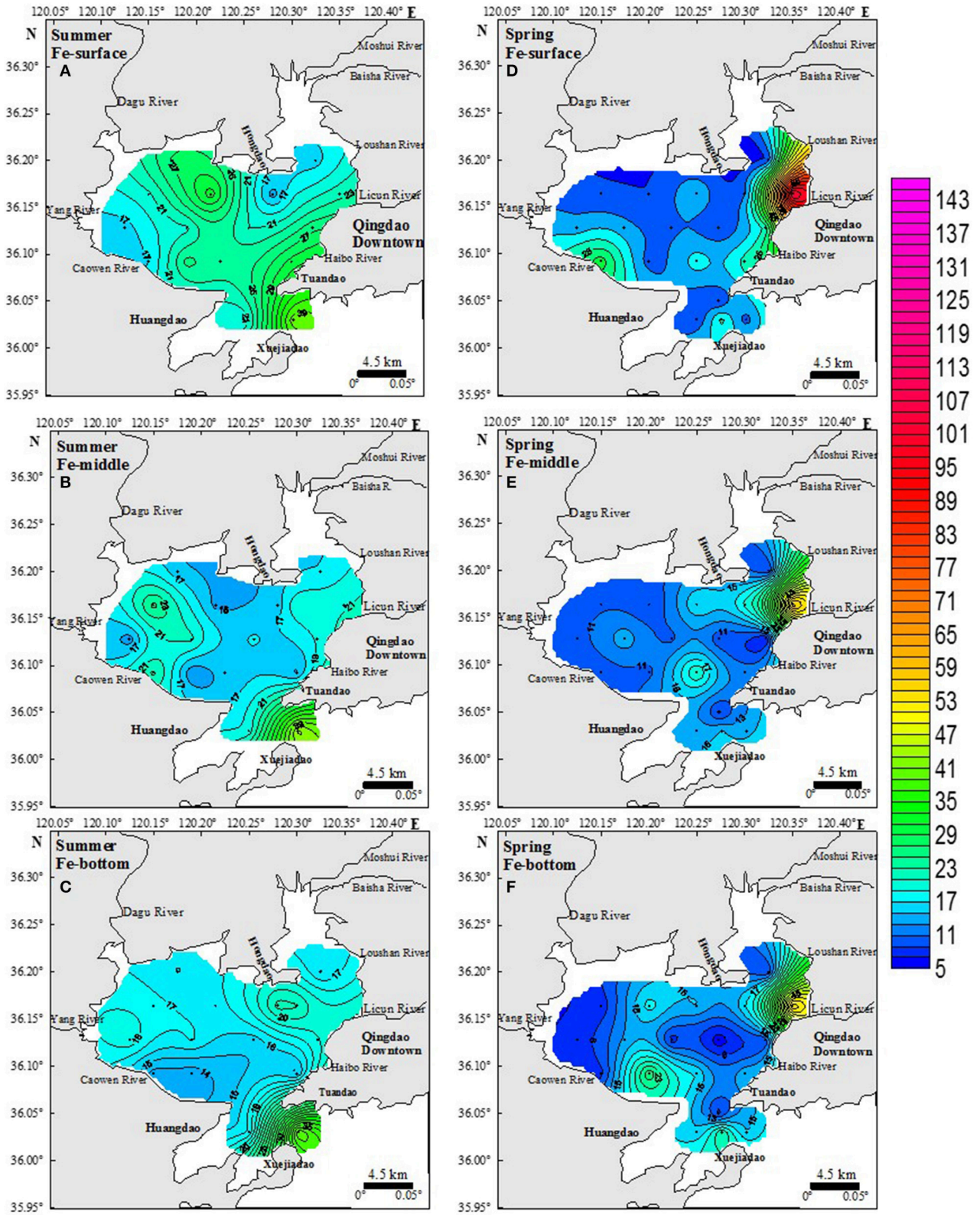

FIGURE 3 | Spatial distribution of DFe concentrations (nM) in summer (A–C) and spring (D–F) period in three layers. The color scale represented the DFe concentrations. All panels use the same color scale.

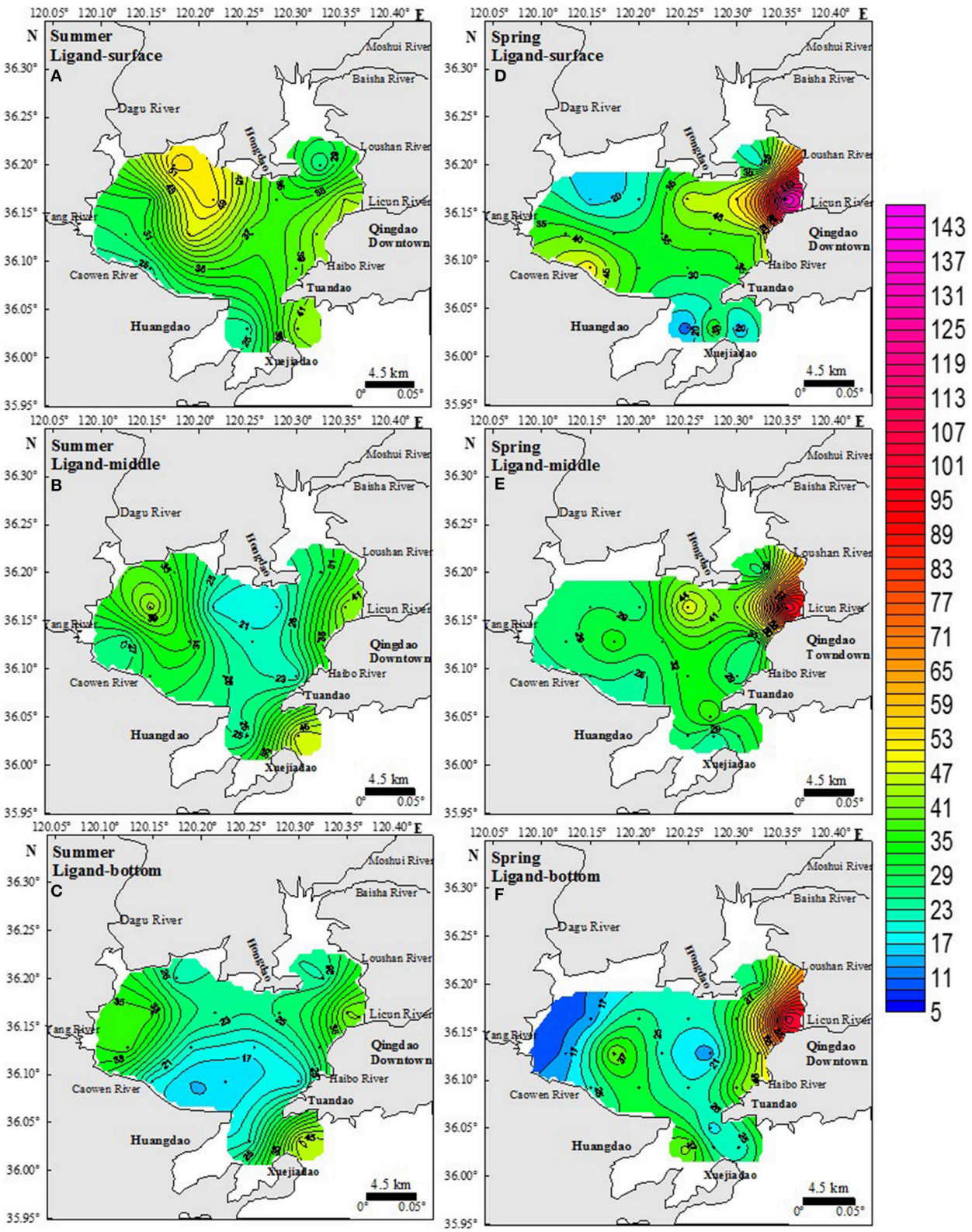

FIGURE 4 | Spatial distribution of ligand concentrations (nM) in summer (left side) and spring periods (right side) in surface (A,D), middle (B,E), and bottom (C,F) seawater layers. The color scale represented the L_t concentrations. All panels use the same color scale as the color scale of DFe concentration in **Figure 3**.

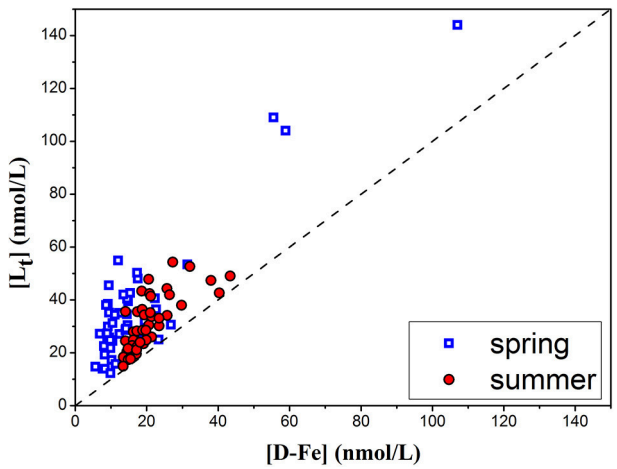

FIGURE 5 | Total ligand (L_t) concentrations as a function of DFe for spring (blue squares) and summer (red circles) periods. The dashed black line represents 1:1 line.

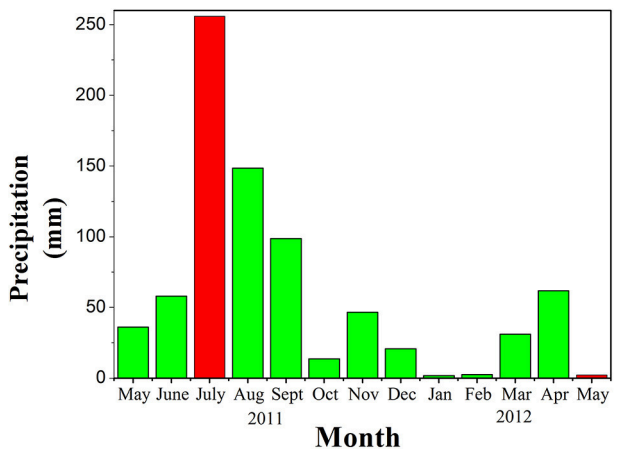

FIGURE 6 | Monthly precipitation in the urban area from May 2011 to May 2012. The data were obtained from the Qingdao statistical yearbook (http://www.stats-qd.gov.cn/statsqd/Columns/tjnjx.shtml) in 2011 and 2012. Red bars represent our sampling months; green bars represent other months.

Figure 7 shows the residual current in the JZB after building the cross-bay bridge (completed on June, 2011). The tidal current in the JZB is classified as a regular semidiurnal tidal current (Li et al., 2014). As seen in **Figure 7**, many circulations of residual current were observed in the inner JZB, and more residual currents appeared in summer than in spring (He et al., 2013). This may result in better vertical and horizontal uniformity of [DFe] in summer, compared to spring. The residual current in the eastern JZB hindered the diffusion of pollutants to the middle and western JZB (**Figure 7**); therefore, the DFe-values in the eastern JZB were higher than in the middle and the western JZB (Li et al., 2014). In addition, because of residual currents north of Huangdao, DFe may be partly enriched and its diffusion hindered into the rest of the JZB (**Figure 7**); hence, high DFe concentrations were observed there in spring and in summer. Being influenced by tide, residual circulation and wind, hydrodynamic force of the JZB is complex and may significantly influence the migration and diffusion of DFe (**Figure 7**).

The water exchange capacity (WEC) of the JZB is an apparent phenomenon from residual currents and have significant spatial differences (Liu et al., 2004). According to Lü et al. (2010)'s study about WEC, two regions were observed to have the weakest WEC, the west-southwestern part and the most northeastern part of the JZB, which has water residence time longer than 80 days due to a weak WEC (Lü et al., 2010). Therefore, the DFe of these two regions (the northwest of the Huangdao Island and at the Caowen River estuary) could be accumulate to high concentrations in spring and in summer (**Figure 3**).

The Iron Biogeochemical Cycle in JZB

Sources and Removal of DFe

The highest DFe concentrations were measured at Licun River estuary in the eastern area of the JZB, especially in spring (**Figure 3**). Spring is a dry season in Qingdao area (**Figure 6**). Most of the rivers that are located in the eastern part of the bay (Licun, Haibo, and Loushan Rivers (He et al., 2013) are highly polluted with industrial wastewater and domestic sewage that contain DFe. The sewage treatment plants along the eastern side of the JZB (**Figure 2**), release $\sim 1.14 \times 10^6$ t/d of waste water into the JZB (Qingdao Bureau of Statistics, 2014). The western part of the JZB is an agricultural area, with lower wastewater discharge containing DFe, especially in spring (**Figure 3**).

Summer season is the wet season in Qingdao area. The annual rain fall mainly occurs in July. As a result, the river input to the JZB is higher than in spring, especially in the western area of the JZB. In the ES, however, the concentration of DFe in rain water (75 nM, unpublished data) was lower than in waste water. So comparing to spring, the DFe concentration decreased at Licun River estuary due to the dilution of rivers entering into the bay with rain water. However, in the western bay (NWS region), rivers in summer carry higher flux of fresh water into the JZB than that in spring, especially the Dagu (~177% of all annual river runoff to the JZB, Sheng et al., 2014), but also Yang and Caowen Rivers (**Figure 6**, Sheng et al., 2014). Fresh water in rivers has high DFe concentration (Wang and Liu, 2003; Stolpe et al., 2010) and would increase DFe in the seawater. Our results showed that the DFe concentration in the NWS region in summer was much higher than that in spring (**Figure 3**), indicating that rivers that flow through agricultural regions are sources of DFe in the NWS region. It seems to be a net effect of source and removal of DFe (will be discussed later), but generally indicating lower influence from agricultural impacts than from industrial ones on the DFe concentration in the JZB.

Rainfall not only increased the discharge of rivers, but also directly increased the DFe concentration in the JZB seawater. In general, the DFe concentrations in summer were much higher than those in spring, which may be caused by the input of rainwater (**Table 1**, **Figure 6**). Our summer campaign (July 19, 2011) was conducted just after the highest rainfall event of that

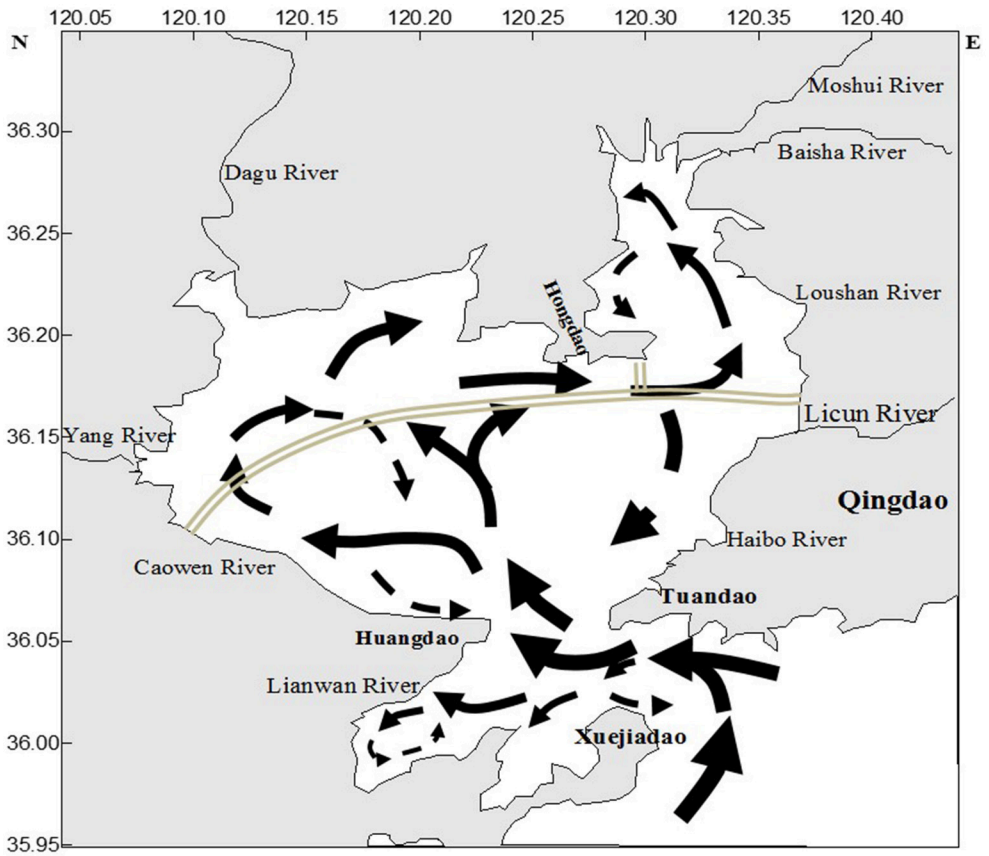

FIGURE 7 | The residual current in the JZB after building the cross-bay bridge (Aug, 2012). The double lines represent the cross bridge; the arrows symbolize the direction of residual current in the JZB. The data are from Li et al. (2014).

year (July 2–4, 2011), which induced a strong disturbance and mixing among different regions (**Figure 6**, Qingdao statistical yearbook in 2011 and 2012[2]). Additionally, strong rain causing flood events, brought terrigenous sewage/water through rivers entering into the bay, which caused an increase of the DFe concentration. In the central bay, which was less influenced by the input of wastewater than the ES and NWS region, higher DFe concentration of surface water in summer than in spring was detected (**Figure 3**). This was the influence of direct input of rainwater. High DFe concentrations of the JZB water cannot easily drain out from the bay and exchange with Yellow Sea, causing a long residence time of DFe (**Figure 7**).

Removal of DFe from the JZB is particularly noticed at the entrance of the bay, where from summer to spring there was a significant decrease in dissolved iron concentration (**Figure 3**), indicating that water exchange with the Yellow sea occurred. However, especially in the coastal areas of the bay, the removal of DFe is ascribed to consumption by the biota which is eventually, by degradation and sinking, eliminated from the water column. Seasonal differences of temperature and nutrients concentration corroborate this hypothesis. It is known that a growth of phytoplankton and bacteria requires the uptake of available Fe from the seawater (Brand et al., 1983; Hutchins et al., 1999). According to Wang (2013) in his study of phytoplankton in the JZB, phytoplankton cell abundance and chlorophyll *a* in spring were higher than in summer (Wang, 2013). Sufficient nutrients in the NWS region supported the growth of phytoplankton and as a result, the uptake of the DFe causing lowering of DFe, which was noticed on the plumes of these two rivers. During spring blooms (February) in the JZB, the DFe concentrations decreased significantly (Schoemann et al., 1998). Our results with the DFe concentrations in the NWS region in summer being higher than that in spring (**Figure 3** and **Table 1**) corroborated Wang's study. The amount of phytoplankton in spring was larger than in summer (Wang, 2013), and these phytoplankton and zooplankton metabolites apparently have taken up available iron and decreased the DFe concentrations. Consequently, DFe in the NWS region decreased more than in the ES region, and in the NWS region it was higher in summer than in spring (**Figure 3** and **Table 1**). Furthermore, suspended particles in seawater adsorb Fe attached to particulate organic functional groups (de Baar and de Jong, 2001), and so decrease the concentration of DFe [in the JZB, the organic suspended particles (OSP) make up more than a half of suspended particles, especially in the south

[2]*Statistical Bureau of Qingdao*. Available online at: http://www.stats-qd.gov.cn (in Chinese).

of the JZB due to the port of Qingdao near station D4 (Bi et al., 2007)]. Due to the impact of tide, some OSP would be swept out by the seawater, and the DFe would be released again, resulting in high DFe concentrations of the CSS region in summer (**Figure 3**).

Iron-complexing Organic Ligands

An excess of organic ligands over DFe concentrations was observed in both spring and summer periods, which indicated that DFe in the JZB existed mostly in the form of strong organic complexes (**Table 1**) that play a governing role in maintaining iron in dissolved state. This observation is expected and is consistent with previous CLE-aCSV studies, such as in the open ocean surface waters and coastal waters (Rue and Bruland, 1995; Boye et al., 2001, 2003; Powell and Wilson-Finelli, 2003; Buck and Bruland, 2007; Buck et al., 2007).

In spring, the highest [L_t] was observed near the estuary of the Licun River in the ES region and was ascribed to constant riverine inputs from industry and domestic wastewater associated with the slow water exchange (dilution factor) in the ES region (**Figure 4**). These wastewaters contained high concentrations of dissolved organic matter (DOM), polychlorinated biphenyl, protein-like and humic-like component, etc. (Guo et al., 2011; Lu et al., 2014), which might be a part of L_t. Furthermore, the L_t concentrations in this region (Industrial region) in spring were higher than that in the NWS region (agricultural region; **Figure 4**). It directs us toward the conclusion that L_t has a more industrial source than an agricultural source.

Our results also show that the L_t concentration of the NWS region in summer was much higher than in spring (**Figure 4** and **Table 1**). This was because the rainfall brought a large amount of organic pesticide and humic substances (HS) from the farmland into the Dagu and Yang Rivers in the NWS region. Hexachlorocyclohexane soprocide (HCH, Yang et al., 2011) and dichloro diphenyl trichloroethane (DDT, Peng et al., 2014) contamination were reported in this area. These organic pesticides may complex with DFe and become one kind of ligand because of carboxylic, hydroxyl and phenolic functional groups (Nuzzo et al., 2013). According to the study of HS in the JZB, Dagu River was an important source of HS in the JZB (Ji et al., 2006). Laglera and van den Berg's study has given some evidence that L_t was partly composed of humic substances (HS; Laglera et al., 2007; Laglera and van den Berg, 2009), as well as studies of Jones and Bundy (Jones et al., 2011; Bundy et al., 2014). Also, HS derived terrestrial inputs have been found in coastal as well as in deep waters, contributing to the pool of Fe-binding ligands (Laglera and van den Berg, 2009; Bundy et al., 2014). During irrigating of farmlands and heavy rainfall, soil is carried into river water and then into the whole JZB. It matches with the hypothesis that river water entering into NWS region was a source of L_t. Therefore, in the NWS, irrigating activities in combination with rain impact L_t concentrations.

On the other hand, the seasonal variation of L_t in the CSS region was smaller than that of the ES region (spring>summer, **Figure 4**). However, the CSS region, being in the middle of the bay, was less influenced by terrestrial sources than the ES and the NWS regions.

In the combination with the influence by the industry and agriculture, regular annual phytoplankton blooms and protozoan grazing in the JZB would increase %FeL, like lipophilic endogenic cellular exudates such as dissolved free and combined amino acids (Nagata and Kirchman, 1991; Öztürk et al., 2002). From May (spring campaign) to July (summer campaign) phytoplankton blooms in the JZB may be mainly limited by phosphate (PO_4–P; Guo et al., 2012). In spring, the highest total dissolved phosphorus concentrations (TDP) were observed at stations A2 and B5 in the ES region (**Table 2**), which was impacted by terrestrial input. The TDP in these areas increased the growth of phytoplankton (Chen et al., 2012b; Guo et al., 2012). It is to be presumed that iron organic ligands and their excess were produced during degradation of dead cells and released during grazing, thus these ligands would stabilize high DFe concentration (Gerringa et al., 2006). The L_t is related to the TDP-values which matches with the highest DFe-values observed in that region (**Figures 3**, **4**). The NWS region (where nutrients were used up after the spring bloom) and the CSS region (with a few terrestrial sources and strong WEC) were characterized with limited phytoplankton growth in spring, which was indicated by low L_t concentrations and also low DFe-values (**Table 1** and Guo et al., 2012).

The logK′-values in the spring samples were weaker than in the summer ones (**Table 1**). Though it isn't clearly known what forms weak ligands, previous studies have implied that they may be a combination of degraded cellular material from seawater (Hunter and Boyd, 2007), like polysaccharides (Hassler et al., 2011), thiols, and heme (Hopkinson et al., 2008).

Iron Speciation and Bioavailability

Iron limitations on phytoplankton growth may occur even though the DFe-value is abundant (Nagai et al., 2007). The JZB is eutrophic and has had outbreaks of red tides every year since 1997. Diatoms, such as Skeletonemacostatum, are the dominant species in the JZB, whereas cyanobacteria such as *Synechococcus* spp. were low (average 4.7%) among the total biomass of phytoplankton in the JZB (Wu et al., 2005; Zhao et al., 2005). These phenomena may be influenced by low available iron in the JZB. Although high iron concentrations were observed in the JZB, almost all of DFe was complexed by organic ligands (**Table 1**). On average, higher conditional stability constants in summer than in spring remind us on possible formation of colloidal inert iron (Gledhill and Buck, 2012).

Variation of DFe and L_t in the Two Contrasting Periods

Variations of DFe between summer and spring period were observed (**Figures 3–5**). The average concentrations of DFe in summer were higher than in spring. The reasons that account for this difference were direct wet deposition from rain water as well as the increased river input from larger amounts of rainfall in summer. The rainfalls in summer and spring were 256 and 2.2 mm, respectively (**Figure 6**). In summer, direct rain input and the reaction of drainage from land to rivers and their estuaries increased nutrients in the JZB, as well as dissolved iron, also shown by other authors (Wang, 2013). However, less

variations of L_t were observed between two sampling periods than that of DFe. The possible reason for this might be mainly dissolved iron coming from rain fall in summer that increased total iron concentrations in the JZB, but also iron consumed by phytoplankton in the spring period that deceased its dissolved fraction. These results can be corroborated by the increased ratio of [L_t] to [DFe] from summer to spring. The average ratio of [L_t] to [DFe] of the NWS, ES, and CSS in spring were higher than that in summer (**Table 1**). According to Willey's study (Willey et al., 2000) inorganic Fe species were found to dominate in rainwater at pH from 4.0 to 5.0 [free Fe(II) ion, Fe(III)-oxalate and $Fe(OH)_2^+$].

There are two main mechanisms governing concentration of DFe, one is the input of industrial and rain wastewater, the other is the uptake by organisms. In general, the seasonal variations of DFe were higher than that of L_t (**Figures 3**, **4**; **Table 1**).

CONCLUSION

The studied distribution of DFe, its organic ligands and inorganic Fe during two contrasting spring and summer periods in surface, middle and bottom layers of the JZB indicated that DFe of the NWS, ES and CSS regions was mostly influenced by agriculture, industrial, and domestic wastewater, and tides, respectively. The influence from industrial and domestic wastewater was much stronger than the influence from agriculture. The riverine and rainfall contribution to input of iron into the shallow JZB regularly, season-dependent, increases the DFe concentrations. Iron-complexing organic ligands were represented by one class of ligands with seasonal dependent stability constants, stronger in summer period. They greatly exceeded the DFe concentration, so they played a governing role in maintaining iron in the water column in both contrasting periods. The L_t is related to TDP-values, while [L_t]/[DFe] ratio seems to be affected by rain season in summer and by biomass production in spring.

Additional data collection and analyses are envisaged in order to corroborate the main processes governing iron distribution and speciation proposed in this study.

AUTHOR CONTRIBUTIONS

RY designed experiments; RY, SW and YL collected samples; RY, HS, SW and YL carried out experiments; RY, HS and SW analyzed experimental results; RY, HS, IP and DO analyzed data and developed analysis tools; RY, HS, IP and DO wrote the manuscript.

ACKNOWLEDGMENTS

This work was financially supported by the National Science Foundation of China (all awarded to RY, 41140037, 41276069), the Young Scientist Award Science Foundation of Shandong, China (awarded to RY, BS2010HZ026), the Open Science Funding of the Key Lab of The First Institute of Oceanography, SOA (awarded to RY, MESE-2011-03), and the visiting scholar funding of the Key Laboratory of Physical Oceanography of Ministry of Education, China (awarded to Chunlei Fan). We acknowledge bilateral Chinese-Croatian project "Determination of trace metal speciation in coastal waters: toward developing new criteria for water quality control and risk assessment" (PI RY and IP), that enabled our collaboration. This work is also supported by the Croatian Science Foundation under the project number IP–2014–09–7530–MEBTRACE (PI DO).

REFERENCES

Abualhaija, M. M., Whitby, H., and van den Berg, C. M. G. (2015). Competition between copper and iron for humic ligands in estuarine waters. *Mar. Chem.* 172, 46–56. doi: 10.1016/j.marchem.2015.03.010

Baker, A. R., Kelly, S. D., Biswas, K. F., Witt, M., and Jickells, T. D. (2003). Atmospheric deposition of nutrients to the Atlantic Ocean. *Geophys. Res. Lett.* 30, 2296–2299. doi: 10.1029/2003gl018518

Bi, L., Bai, J., Zhao, Z., Li, Y., and Yun, Z. (2007). Characteristics of suspended particles in summer in Jiaozhou Bay. *Mar. Environ. Sci.* 26, 518–522.

Boyd, P. W., Jickells, T., Law, S., Blain, S., Boyle, E. A., Buesseler, K. O., et al. (2007). Mesoscale iron enrichment experiments 1993-2005: synthesis and future directions. *Science* 315, 612–617. doi: 10.1126/science.1131669

Boye, M., Aldrich, A. P., van den Berg, C. M. G., de Jong, J. T. M., Veldhuis, M., and Baar, H. J. W. (2003). Horizontal gradient of the chemical speciation of iron in surface waters of the northeast Atlantic Ocean. *Mar. Chem.* 80, 129–143. doi: 10.1016/S0304-4203(02)00102-0

Boye, M., van den Berg, C. M. G., de Jong, J. T. M., Leach, H., Croot, P., and de Baar, H. J. M. (2001). Organic complexation of iron in the Southern Ocean. *Deep Sea Res. I* 48, 1477–1497. doi: 10.1016/S0967-0637(00)00099-6

Brand, L. E., Sunda, W. G., and Guillard, R. R. L. (1983). Limitation of marine phytoplankton reproductive rates by zinc, manganese, and iron. *Limnol. Oceanogr.* 28, 1182–1198. doi: 10.4319/lo.1983.28.6.1182

Buck, K. N., and Bruland, K. W. (2007). The physicochemical speciation of dissolved iron in the Bering Sea, Alaska. *Limnol. Oceanogr.* 52, 1800–1808. doi: 10.4319/lo.2007.52.5.1800

Buck, K. N., Lohan, M. C., Berger, C. J. M., and Bruland, K. W. (2007). Dissolved iron speciation in two distinct river plumes and an estuary: implications for riverine iron supply. *Limnol. Oceanogr.* 52, 843–855. doi: 10.4319/lo.2007.52.2.0843

Buesseler, K. O., Doney, S. C., Karl, D. M., Boyd, P. W., Caldeira, K., Chai, F., et al. (2008). Environment: ocean iron fertilization–moving forward in a sea of uncertainty. *Science* 319, 162. doi: 10.1126/science.1154305

Bundy, R. M., Biller, D. V., Buck, K. N., Bruland, K. W., and Barbeau, K. A. (2014). Distinct pools of dissolved iron-binding ligands in the surface and benthic boundary layer of the California current. *Limnol. Oceanogr.* 59, 769–787. doi: 10.4319/lo.2014.59.3.0769

Chen, B., Zhang, Y., Liu, J., and Kong, X. (2012a). Tidal current dynamic characteristic and its relation with suspended sediment concentration in Jiaozhou Bay. *Adv. Mar. Sci.* 30, 24–35 (in Chinese with English abstract).

Chen, C., Yang, G., Gao, X., Yu, J., and Wu, G. (2012b). Nutrients distributional characteristics and eutrophication in the sea-surface microlayer and subsurface water in the Jiaozhou Bay. *Acta Sci. Circum.* 32, 1856–1865 (in Chinese).

Chen, H., Hua, F., Liu, N., and Sun, X. (2009). Study on variability of coastline and water depth of Jiaozhou Bay in recent years. *Adv. Mar. Sci.* 27, 149–154 (in Chinese with English abstract).

Coale, K. H. (2004). Southern ocean iron enrichment experiment: carbon cycling in high- and low-Si waters. *Science* 304, 408–414. doi: 10.1126/science.1089778

Croot, P. L., and Johansson, M. (2000). Determination of iron speciation by cathodic stripping voltammetry in seawater using the competing ligand 2-(2-Thiazolylazo)-p-cresol (TAC). *Electroanalysis* 12, 565–576. doi: 10.1002/(SICI)1521-4109(200005)12:8<565::AID-ELAN565>3.0.CO;2-L

Cullen, J. T., Bergquist, B. A., and Moffett, J. W. (2006). Thermodynamic characterization of the partitioning of iron between soluble and colloidal species in the Atlantic Ocean. *Mar. Chem.* 98, 295–303. doi: 10.1016/j.marchem.2005.10.007

de Baar, H. J., and de Jong, J. T. (2001). "Distributions, sources and sinks of iron in seawater," in *IUPAC Series on Analytical and Physical Chemistry of Environmental Systems, Vol. 7*, eds D. R. Turner and K. A. Hunter (West Sussex: John Wiley & Sons Ltd), 123–254.

Deng, B., Zhang, J., Zhang, G., and Zhou, J. (2010). Enhanced anthropogenic heavy metal dispersal from tidal disturbance in the Jiaozhou Bay, North China. *Environ. Monit. Assess.* 161, 349–358. doi: 10.1007/s10661-009-0751-x

Ding, W. L. (1992). "Tides and tidal currents," in *Ecology and Living Resources of Jiaozhou Bay*, ed R.Y. Liu (Beijing: Science Press), 30–56 (in Chinese).

Gerringa, L. J. A., Blain,. S., Laan, P., Sarthou, G., Veldhuis, M. J. W., Brussaard, C. P. D., et al. (2008). Fe-binding dissolved organic ligands near the Kerguelen Archipelago in the Southern Ocean (Indian sector). *Deep Sea Res. II Top. Stud. Oceanogr.* 55, 606–621. doi: 10.1016/j.dsr2.2007.12.007

Gerringa, L. J. A., Rijkenberg, M. J. A., Wolterbeek, H. T., Verburg, T. G., Boye, M., and de Baar., H. J. W. (2007). Kinetic study reveals weak Fe-binding ligand, which affects the solubility of Fe in the Scheldt estuary. *Mar. Chem.* 103, 30–45. doi: 10.1016/j.marchem.2006.06.002

Gerringa, L. J. A., Veldhuis, M. J. W., Timmermans, K. R., Sarthou, G., and de Baar, H. J. W. (2006). Co-variance of dissolved Fe-binding ligands with phytoplankton characteristics in the Canary Basin. *Mar. Chem.* 102, 276–290. doi: 10.1016/j.marchem.2006.05.004

Gledhill, M., and Buck, K. N. (2012). The organic complexation of iron in the marine environment: a review. *Front. Microbiol.* 3:69. doi: 10.3389/fmicb.2012.00069

Gledhill, M., and van den Berg, C. M. G. (1994). Determination of complexation of iron(III) with natural organic complexing ligands in seawater using cathodic stripping voltammetry. *Mar. Chem.* 47, 41–54. doi: 10.1016/0304-4203(94)90012-4

Grasshoff, K., Kremling, K., and Ehrhardt, M. (1983). *Methods of Seawater Analysis*. New York, NY: John Wiley & Sons.

Guo, F., Zhao, J., Chen, J. F., Chen, B. J., Liu, C. X., and Zhang, Y. (2012). Nitrogen and phosphorous pollution in shellfish culture area of Jiaozhou Bay. *Prog. Fishery Sci.* 33, 116–122 (in Chinese with English abstract).

Guo, J., Yin, Y., Zheng, L., Yu, W., Zhao, H., and Yang, D. (2011). The distribution and risk assessment of polychlorinated biphenyl in surface sediments in estuaries of Jiaozhou Bay, China. *J. Agro Environ. Sci.* 30, 965–972 (in Chinese).

Hassler, C. S., Alasonati, E., Mancuso Nichols, C. A., and Slaveykova, V. I. (2011). Exopolysaccharides produced by bacteria isolated from the pelagic Southern Ocean—Role in Fe binding, chemical reactivity, and bioavailability. *Mar. Chem.* 123, 88–98. doi: 10.1016/j.marchem.2010.10.003

He, S., Li, G., and Shi, J. (2013). Distribution of heavy metals in surficial sediments of Jiaozhou Bay and its influencing factors. *Mar. Geol. Front.* 29, 41–48 (in Chinese with English abstract). doi: 10.16028/j.1009-2722.2013.04.005

Hider, R. C., and Kong, X. (2010). Chemistry and biology of siderophores. *Nat. Prod. Rep.* 27, 637–657. doi: 10.1039/b906679a

Hopkinson, B. M., Roe, K. L., and Barbeau, K. A. (2008). Heme uptake by Microscilla marina and evidence for heme uptake systems in the genomes of diverse marine bacteria. *Appl. Environ. Microbiol.* 74, 6263–6270. doi: 10.1128/AEM.00964-08

Hudson, R. J., and Morel, F. M. (1993). Trace metal transport by marine microorganisms, implications of metal coordination kinetics. *Deep Sea Res. I Oceanogr. Res. Pap.* 40, 129–150. doi: 10.1016/0967-0637(93)90057-A

Hunter, K. A., and Boyd, P. W. (2007). Iron-binding ligands and their role in the ocean biogeochemistry of iron. *Environ. Chem.* 4, 221–232. doi: 10.1071/EN07012

Hutchins, D. A., Witter, A. E., Butler, A., and Luther, G. W. (1999). Competition among marine phytoplankton for different chelated iron species. *Nature* 400, 858–861. doi: 10.1038/23680

Ji, N. Y., Zhao, W. H., Wang, J. T., and Miao, H. (2006). Change of Humic-like fluorescence characteristics of dissolved organic matter from Dagu River to Jiaozhou Bay. *Environ. Sci.* 27, 1073–1077 (in Chinese with English abstract).

Jones, M. E., Beckler, J. S., and Taillefert, M. (2011). The flux of soluble organic-iron (III) complexes from sediments represents a source of stable iron (III) to estuarine waters and to the continental shelf. *Limnol. Oceanogr.* 56, 1811–1823. doi: 10.4319/lo.2011.56.5.1811

Kieber, R. J., Williams, K., Willey, J. D., Skrabal, S., and Avery, G. B. (2001). Iron speciation in coastal rainwater, concentration and deposition to seawater. *Mar. Chem.* 73, 83–95. doi: 10.1016/S0304-4203(00)00097-9

Kremling, K., Tokos, J. J. S., Brugmann, L., and Hansen, H. P. (1997). Variability of dissolved and particulate trace metals in the Kiel and Mecklenburg bights of the Baltic Sea, 1990-1992. *Mar. Pollut. Bull.* 37, 15–27. doi: 10.1016/s0025-326x(96)00060-4

Kuma, K., Nishioka, J., and Matsunaga, K. (1996). Controls on iron (III) hydroxide solubility in seawater: the influence of pH and natural organic chelators. *Limnol. Oceanogr.* 41, 396–407. doi: 10.4319/lo.1996.41.3.0396

Laglera, L. M., Battaglia, G., and van den Berg, C. M. G. (2007). Determination of humic substances in natural waters by cathodic stripping voltammetry of their complexes with iron. *Anal. Chim. Acta* 599, 58–66. doi: 10.1016/j.aca.2007.07.059

Laglera, L. M., and van den Berg, C. M. G. (2009). Evidence for geochemical control of iron by humic substances in seawater. *Limnol. Oceanogr.* 54, 610–619. doi: 10.4319/lo.2009.54.2.0610

Li, P., Li, G., Qiao, L., Chen, X., Shi, J., Gao, F., et al. (2014). Modeling the tidal dynamic changes induced by the bridge in Jiaozhou Bay, Qingdao, China. *Continental Shelf Res.* 84, 43–53. doi: 10.1016/j.csr.2014.05.006

Lin, H., and Twining, B. S. (2012). Chemical speciation of iron in Antarctic waters surrounding free-drifting icebergs. *Mar. Chem.* 128–129, 81–91. doi: 10.1016/j.marchem.2011.10.005

Liu, J., Guo, Z. R., Yuan, X. J., Zhang, B., and Ma, Z. Y. (2014). Temporal and spatial variation of nutrients in the rivers around Jiaozhou Bay and its fluxes into the sea. *Environ. Chem.* 33, 262–268 (in Chinese with English abstract). doi: 10.7524/j.issn.0254-6108.2014.02.014

Liu, S. M., Zhang, J., Chen, H. T., and Zhang, G. S. (2005). Factors influencing nutrient dynamics in the eutrophic Jiaozhou Bay, North China. *Prog. Oceanogr.* 66, 66–85. doi: 10.1016/j.pocean.2005.03.009

Liu, Z., Wei, H., Liu, G., and Zhang, J. (2004). Simulation of water exchange in Jiaozhou Bay by average residence time approach. *Estuar. Coast Shelf Sci.* 61, 25–35. doi: 10.1016/j.ecss.2004.04.009

Lu, J., Sun, S., Zhang, G., and Zhao, Z. (2014). Temporal and spatial variation of fluorescence characteristics of dissolved organic matters during summer of 2011 in Jiaozhou Bay. *Mar. Sci.* 38, 1–6 (in Chinese with English abstract). doi: 10.11759/hykx20130325001

Lü, X. G., Zhao, C., Xia, C. S., and Qiao, F. L. (2010). Numerical study of water exchange in the Jiaozhou Bay and the tidal residual currents near the bay mouth. *Acta Oceanol. Sin.* (in Chinese), 2, 20–30 (in Chinese with English abstract).

Ma, L., Yang, X., Qi, Y., Liu, Y., and Zhang, J. (2014). Oceanic area change and contributing factor of Jiaozhou Bay. *Sci. Gengr. Sin.* 3, 365–369 (in Chinese with English abstract).

Marine Environmental Quality of Qingdao (2014). Available online at: http://ocean.qingdao.gov.cn/n12479801/n32205288/160125182106067781.html

Martin, J. H. (1990). Glacial-interglacial CO2 change, the iron hypothesis. *Paleoceanography* 5, 1–13. doi: 10.1029/PA005i001p00001

Martin, J. H., and Fitzwater, S. E. (1988). Iron deficiency limits phytoplankton growth in the north-east Pacific subarctic. *Nature* 331, 341–343. doi: 10.1038/331341a0

Mawji, E., Gledhill, M., Milton, J. A., Tarran, G. A., Ussher, S., Thompson, A., et al. (2008). Hydroxamate siderophores: occurrence and importance in the Atlantic Ocean. *Environ. Sci. Technol.* 42, 8675–8680. doi: 10.1021/es801884r

Öztürk, M., Bizsel, N., and Steinnes, E. (2003). Iron speciation in eutrophic and oligotrophic Mediterranean coastal waters; impact of phytoplankton and protozoan blooms on iron distribution. *Mar. Chem.* 81, 19–36. doi: 10.1016/S0304-4203(02)00137-8

Morel, F. M., Hudson, R. J., and Price, N. M. (1991). Limitation of productivity by trace metals in the sea. *Limnol. Oceanogr.* 36, 1742–1755. doi: 10.4319/lo.1991.36.8.1742

Öztürk, M., Steinnes, E., and Sakshaug, E. (2002). Iron Speciation in the Trondheim Fjord from the perspective of iron limitation for phytoplankton. *Estuar. Coast Shelf Sci.* 55, 197–212. doi: 10.1006/ecss.2001.0897

Nagai, T., Imai, A., Matsushige, K., Yokoi, K., and Fukushima, T. (2007). Dissolved iron and its speciation in a shallow eutrophic lake and its inflowing rivers. *Water Res*. 41, 775–784. doi: 10.1016/j.watres.2006.10.038

Nagata, T., and Kirchman, D. L. (1991). Release of dissolved free and combined amino acids by bacterivorous marine flagellates. *Limnol. Oceanogr*. 36, 433–443. doi: 10.4319/lo.1991.36.3.0433

Nuzzo, A., Sánchez, A., Fontaine, B., and Piccolo, A. (2013). Conformational changes of dissolved humic and fulvic superstructures with progressive iron complexation. *J. Geochem. Explor*. 129, 1–5. doi: 10.1016/j.gexplo.2013.01.010

Omanović, D., Garnier, C., and Pižeta, I. (2015). ProMCC: an all-in-one tool for trace metal complexation studies. *Mar. chem*. 173, 25–39. doi: 10.1016/j.marchem.2014.10.011

Peng, J., Song, J., Li, C., and Yu, L. (2014). Risk assesment of ingesting polyunsaturated fatty acids and organochlorine pesticide residues in five seaweeds from Jiaozhou Bay. *Oceanol. Limnol. Sin*. 45, 80–87 (in Chinese).

Pižeta, I., Sander, S., Hudson, R., Omanović, D., Baars, O., Barbeau, K., et al. (2015). Interpretation of complexometric titration data: an intercomparison of methods for estimating models of trace metal complexation by natural organic ligands. *Mar. chem*. 173, 3–24. doi: 10.1016/j.marchem.2015.03.006

Poorvin, L., Rinta-Kanto, J. M., and Hutchins, D. A.,(2004). Viral release of iron and its bioavailability to marine plankton. *Limnol. Oceanogr*. 49, 1734–1741. doi: 10.4319/lo.2004.49.5.1734

Powell, R. T., and Wilson-Finelli, A. (2003). Importance of organic Fe complexing ligands in the Mississippi River plume. *Estuar. Coast Shelf Sci*. 58, 757–763. doi: 10.1016/S0272-7714(03)00182-3

Qingdao Bureau of Statistics (2014). *Qingdao Statistical Yeatbook-2013[M]*. Beijing: China Statistics Press.

Redfield, A. C. (1958). The biological control of chemical factors in the environment. *Am. Sci*. 46, 230A, 205–221.

Rue, E. L., and Bruland, K. W. (1995). Complexation of iron(III) by natural organic ligands in the Central North Pacific as determined by a new competitive ligand equilibration/adsorptive cathodic stripping voltammetric method. *Mar. Chem*. 50, 117–138. doi: 10.1016/0304-4203(95)00031-L

Sander, S. G., Tian, F., Ibisanmi, E. B., Currie, K. I., Hunter, K. A., and Frew, R. D. (2015). Spatial and seasonal variations of iron speciation in surface waters of the Subantarctic front and the Otago Continental Shelf. *Mar. Chem*. 173, 114–124. doi: 10.1016/j.marchem.2014.09.001

Schoemann, V., de Baar, H. J. W., de Jong, J. T. M., and Lancelot, C. (1998). Effects of phytoplankton blooms on the cycling of manganese and iron in coastal waters. *Limnol. Oceanogr*. 43, 1427–1441. doi: 10.4319/lo.1998.43.7.1427

Sheng, M., Cui, J., Shi, Q., Li, L., and Deng, Y. (2014). Analysis of sediment discharge characteristics of Rivers in Jiaozhou Bay, Qingdao City. *J. China Hydrol*. 34, 92–96 (in Chinese with English abstract).

Siefert, R. L., Johansen, A. M., and Hoffmann, M. R. (1999). Chemical characterization of ambient aerosol collected during the southwest monsoon and intermonsoon seasons over the Arabian Sea, Labile-Fe (II) and other trace metals. *J. Geophys. Res*. 104, 3511–3526. doi: 10.1029/1998JD100067

Stolpe, B., Guo, L., Shiller, A. M., and Hassellöv, M. (2010). Size and composition of colloidal organic matter and trace elements in the Mississippi River, Pearl River and the northern Gulf of Mexico, as characterized by flow field-flow fractionation. *Mar. Chem*. 118, 119–128. doi: 10.1016/j.marchem.2009.11.007

Su, H., Yang, R., Zhang, A., and Li, Y. (2015). Dissolved iron distribution and organic complexation in the coastal waters of the East China Sea. *Mar. Chem*. 173, 208–221. doi: 10.1016/j.marchem.2015.03.007

Sunda, W. G., Swift, D. G., and Huntsman, S. A. (1991). Low iron requirement for growth in oceanic phytoplankton. *Nature* 351, 55–57. doi: 10.1038/351055a0

Sundby, B., Anderson, L. G., Hall, P. O. J., Iverfeldt, A., van der Loeff, M. M. R., and Westerlund, S. F. G. (1986). The effect of oxygen on release and uptake of cobalt, manganese, iron and phosphate at the sediment-water interface. *Geochim. Cosmochim. Acta* 50, 1281–1288. doi: 10.1016/0016-7037(86)90411-4

Tan, S., Shi, G., and Wang, H. (2012). Long-range transport of spring dust storms in Inner Mongolia and impact on the China seas. *Atmos. Environ*. 46, 299–308. doi: 10.1016/j.atmosenv.2011.09.058

Thuróczy, C., Gerringa, L., Klunder, M. B., Middag, R., Laan, P., Timmermans, K. R., et al. (2010). Speciation of Fe in the Eastern North Atlantic Ocean. *Deep Sea Res. Part I Oceanogr. Res. Pap*. 57, 1444–1453. doi: 10.1016/j.dsr.2010.08.004

Tsunogai, S., and Uematsu, M. (1978). Particulate manganese, iron and aluminum in coastal water, Funka Bay, Japan. *Geochem. J*. 12, 39–46. doi: 10.2343/geochemj.12.39

van den Berg, C. M. (1995). Evidence for organic complexation of iron in seawater. *Mar. Chem*. 50, 139–157. doi: 10.1016/0304-4203(95)00032-M

van den Berg, C. M. G. (2006). Chemical speciation of iron in seawater by cathodic stripping voltammetry with dihydroxynaphthalene. *Anal. Chem*. 78, 156–163. doi: 10.1021/ac051441+

Wang, W. (2013). *The Influence of Tyhoon-Induced Precipitation on the Supplementary of Biogenic Elements, the Abundance and Structure of Phytoplankton in Jiaozhou Bay*. Thesis 93, Ocean University of China (in Chinese and English abstract).

Wang, Z., and Liu, C. (2003). Distribution and partition behavior of heavy metals between dissolved and acid-soluble fractions along a salinity gradient in the Changjiang Estuary, eastern China. *Chem. Geol*. 202, 383–396. doi: 10.1016/j.chemgeo.2002.05.001

Willey, J. D., Kieber, R. J., Williams, K. H., Crozier, J. S., Skrabal, S. A., and Avery, G. B. (2000). Temporal variability of iron speciation in coastal rainwater. *J. Atmos. Chem*. 37, 185–205. doi: 10.1023/A:1006421624865

Witter, A. E., Hutchins, D. A., Butler, A., and Luther, G. W. III. (2000). Determination of conditional stability constants and kinetic constants for strong model Fe-binding ligands in seawater. *Mar. Chem*. 69, 1–17. doi: 10.1016/S0304-4203(99)00087-0

Wu, J., and Luther, G. W. III. (1995). Complexation of Fe (III) by natural organic ligands in the Northwest Atlantic Ocean by a competitive ligand equilibration method and a kinetic approach. *Mar. Chem*. 50, 159–177. doi: 10.1016/0304-4203(95)00033-N

Wu, Y. L., Sun, S., and Zhang, Y. S. (2005). Long-term change of environment and its influence on phytoplankton community structure in Jiaozhou Bay. *Oceanol. Limnol. Sin*. 36, 487–498 (in Chinese with English abstract).

Yang, D., Ding, Z., Zheng, L., Bu, Z., and Shi, Q. (2011). Homogeneity of HCH distribution in the Jiaozhou Bay waters. *Coast. Eng*. 30, 66–74 (in Chinese with English abstract).

Zhao, S. J., Xiao, T., Li, H. B., and Xu, J. H. (2005). Distribution of *Synechococcus* spp. in Jiaozhou Bay. *Oceanol. Limnol. Sin*. 36, 534–540 (in Chinese with English abstract).

Zhu, M., Hao, X., Shi, X., Yang, G., and Li, T. (2012). Speciation and spatial distribution of solid-phase iron in surface sediments of the East China Sea continental shelf. *Appl. Geochem*. 27, 892–905. doi: 10.1016/j.apgeochem.2012.01.004

Conflict of Interest Statement: The authors declare that the research was conducted in the absence of any commercial or financial relationships that could be construed as a potential conflict of interest.